International Journal of Engineering

Journal Homepage: www.ije.ir

Development of a New Backward Directional Coupler Based on Perforated Substrates

H. Karimian-Sarakhs, M. H. Neshati*

Department of Electrical Engineering, Ferdowsi University of Mashhad, Mashhad, Iran

PAPER INFO

Paper history:
Received 27 July 2022
Received in revised form 2 December 2022
Accepted 04 December 2022

Keywords:
Directional Coupler
Perforated Substrate
Transmission Matrix

ABSTRACT

In this paper, two wideband 10 dB backward directional couplers based on artificial perforated substrates over the frequency range of 25-35 GHz and 32-38 GHz are developed. An analytical method is proposed to design the coupler geometrical parameters. The theoretical modeling is established based on the coupled version of the transmission line (TL) theory using the extended version of the *ABCD* matrix for four ports microwave network. It is shown that using the proposed method, all required parameters of the directional coupler are determined using the per-unit-length of the applied lines. The geometrical parameters of primary designed couplers are optimized using the particle swarm optimization (PSO) procedure to improve the performance of couplers. The designed couplers are also simulated using High Frequency Structure Simulator (HFSS) software. Moreover, sensitivity analysis is carried out to investigate the effect of fabrication imperfections of the proposed couplers. The obtained results show that the simulated results agree well with the theoretical ones and a low insertion loss (*IL*) with high return loss is obtained over a wide frequency range bandwidth.

doi: *10.5829/ije.2023.36.02b.11*

1. INTRODUCTION

Directional couplers are developed as passive microwave structures consisting of three or four ports designed for arbitrary power dividing ratios, which have been used in various microwave systems including communication and measurement systems [1-5].

So far, a wide variety of waveguide or transmission line-based couplers have been developed and characterized providing a few advantages and disadvantages. Cao et al. [6] designed a directional coupler based on substrate-integrated waveguide (SIW) and stripline techniques; in which TE_{10} and TEM modes can be simultaneously transmitted. However, the operating bandwidth is only about 15%, and its size is too large. Ali et al. [7] designed a hybrid directional coupler based on the printed ridge gap waveguide (PRGW). The most important feature of the proposed coupler includes low signal distortion, low loss, and low size, meanwhile, it provides a limited bandwidth. A two-hole directional coupler consisting of different dielectric-loaded SIWs is introduced for Ka-band by Parment et al. [8]. This coupler provides a very good insertion loss lower than 0.3 dB, and the coupling factor is 20 dB with a flatness of 0.25 dB, but it can be only used for applications with high coupling. Zarifi et al. [9] introduced a variable coupling directional coupler based on a double-layer groove gap waveguide. The coupler size is very large, and also, a low coupling factor cannot be achieved using the proposed coupler. A wideband directional coupler using a dielectric overlay is presented by Peláez-Pérez et al. [10], which provides 15 dB coupling with a maximum flatness of 1 dB.

A 3 dB directional coupler based on periodic vias and multi-holes SIW is developed by Tavakoli and Mallahzadeh [11]. In order to achieve wide bandwidth, several sections are serially connected. However, insertion loss and flatness of the coupling factor are extremely affected by using the multi-holes technique, and these are about 5 dB and 2 dB, respectively. Zhao et al. [12] introduced a compact coupler with a symmetrical square feed for operating at Ka-band. Although the coupler flatness is about 0.5 dB, it provides a very low

*Corresponding Author Institutional Email: neshat@um.ac.ir
(M. H. Neshati)

Please cite this article as: H. Karimian-Sarakhs, M. H. Neshati, Development of a New Backward Directional Coupler Based on Perforated Substrates, ***International Journal of Engineering, Transactions B: Applications***, Vol. 36, No. 02, (2023), 311-320

bandwidth of 7%. Moreover, its insertion loss is as high as 7 dB with the port's isolation around 10 dB.

Tabatabaeian et al. [13] designed a forward-wave directional coupler using periodic patterned ground structure in microstrip coupled lines with a 96% bandwidth, while the coupling flatness is 1 dB and return loss is not better than 10 dB. Tabatabaeian et al. [14] proposed a directional coupler using periodic shunt short-circuited stubs. Although this coupler is compact and the ripple of the final responses is about 1 dB, it shows a very low bandwidth of about 11.7%.

In this paper, an analytical procedure is proposed to design a backward directional coupler based on the coupled version of transmission line (TL) equations. The modified *ABCD* matrix of a four ports microwave network is developed and it is shown that using the introduced matrix, any multi-sections coupled structures can be analyzed. Using the proposed model, the important parameters of a directional coupler, including insertion loss, return loss, coupling level, and isolation factor are determined closed-form expressions are developed for these parameters. Then, two microstrip directional couplers based on one and the two-dimensional perforated substrate is designed. The designed coupler covers the frequency range of 25-35 GHz and 32-38 GHz with a 10 dB coupling level, a maximum flatness of 0.5 dB, and a return loss (*RL*) better than 15 dB. The simulated results show that the fractional bandwidth of the couplers is about 17% and 34%.

2. THEORETICAL MODELLING

A single-section coupled line coupler is shown in Figure 1. In the general case, this four-port coupler is terminated by impedances Z_L, Z_N, and Z_F at three different ports, and driven with a voltage source V_S and internal impedance Z_S at the exciting port.

It is assumed that the coupled lines convey Quasi-TEM waves. Therefore, based on TL theory, the current waves along the lines are given by equations (1a) and (1b) [15], in which I_{10}, I_{20}, and γ are the amplitude of propagating waves of the lines at z=0, and propagation constant given by $\gamma=\alpha+j\beta$, and α, β are the attenuation and phase constant, respectively.

$$I_1(z) = I_{10}\cosh(\gamma z) + k_1 \sinh(\gamma z) \tag{1a}$$

$$I_2(z) = I_{20}\cosh(\gamma z) + k_2 \sinh(\gamma z) \tag{1b}$$

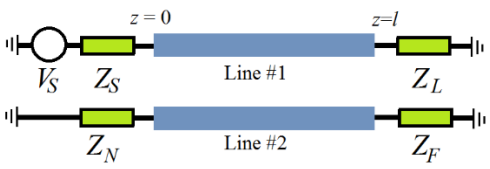

Figure 1. The geometry of a directional coupler

Also, k_1 and k_2 are constant parameters related to the amplitude of the waves of the two lines at $z=l$, respectively given by Equations (2a) and (2b), in which I_{1l}, I_{2l} are the value of the current waves of the two lines at $z=l$, respectively.

$$k_1 = \frac{I_{1l} - I_{10}\cosh(\gamma l)}{\sinh(\gamma l)} \tag{2a}$$

$$k_2 = \frac{I_{2l} - I_{20}\cosh(\gamma l)}{\sinh(\gamma l)} \tag{2b}$$

The corresponding voltage waves propagating on the lines are also determined using the coupled version of TL modeling given by Equations (3a) and (3b) [16].

$$I_1'(z) = -Y_1 V_1(z) + Y_m V_2(z) \tag{3a}$$

$$I_2'(z) = -Y_2 V_2(z) + Y_m V_1(z) \tag{3b}$$

in which

$$Y_1 = G_1 + j\omega C_1 \tag{4a}$$

$$Y_2 = G_2 + j\omega C_2 \tag{4b}$$

$$Y_m = -G_m - j\omega C_m \tag{4c}$$

C_1, C_2, C_m, ω are self and mutual per-unit-length capacitance, and angular frequency, respectively. Also, G_1, G_2, and G_m show self and mutual per-unit-length conductance. By substituting the derivatives of Equation (1) into Equation (3), the voltage waves can be expressed by the following equations.

$$-Y_1 V_1(z) + Y_m V_2(z) = \gamma I_{10}\sinh(\gamma z) + \gamma k_1 \cosh(\gamma z) \tag{5a}$$

$$-Y_2 V_2(z) + Y_m V_1(z) = \gamma I_{20}\sinh(\gamma z) + \gamma k_2 \cosh(\gamma z) \tag{5b}$$

Here, it is desired to extend using the *ABCD* matrix for a 4-port coupled structure as shown in Figure 1. To this end, Equations (6a) and (6b) is defined, in which **T** is a 4×4 matrix of the coupled transmission line.

$$\begin{bmatrix} V_{10} \\ I_{10} \\ V_{20} \\ I_{20} \end{bmatrix} = \mathbf{T} \begin{bmatrix} V_{1l} \\ I_{1l} \\ V_{2l} \\ I_{2l} \end{bmatrix} \tag{6a}$$

$$\mathbf{T} = [T_{nm}]_{4\times 4} \tag{6b}$$

Also, pairs (V_{n0}, I_{n0}), (V_{nl}, I_{nl}); n=1, 2 show that the value of voltage and current for the input port at z=0, and the

output port at $z=l$, and l is the length of the coupled lines, respectively. Using four Equations (1), (2), (5) and (6) the components of matrix **T** are obtained.

$$\mathbf{T}=\begin{bmatrix}\mathbf{T}_{11} & \mathbf{T}_{12}\\ \mathbf{T}_{21} & \mathbf{T}_{22}\end{bmatrix} \tag{7a}$$

$$\mathbf{T}_{11}=\begin{bmatrix}\cosh\gamma l & \frac{\gamma Y_2}{\Delta}\sinh\gamma l\\ \frac{Y_1}{\gamma}\sinh\gamma l & \cosh\gamma l\end{bmatrix} \tag{7b}$$

$$\mathbf{T}_{12}=\begin{bmatrix}0 & \frac{\gamma Y_m}{\Delta}\sinh\gamma l\\ \frac{-Y_m}{\gamma}\sinh\gamma l & 0\end{bmatrix} \tag{7c}$$

$$\mathbf{T}_{21}=\begin{bmatrix}0 & \frac{\gamma Y_m}{\Delta}\sinh\gamma l\\ \frac{-Y_m}{\gamma}\sinh\gamma l & 0\end{bmatrix} \tag{7d}$$

$$\mathbf{T}_{22}=\begin{bmatrix}\cosh(\gamma l) & \frac{\gamma Y_1}{\Delta}\sinh(\gamma l)\\ \frac{Y_2}{\gamma}\sinh(\gamma l) & \cosh(\gamma l)\end{bmatrix} \tag{7e}$$

$$\Delta=Y_1Y_2-Y_m^{\,2} \tag{7f}$$

After specifying matrix **T**, the value of voltage and current of the coupled lines at four ports have to be calculated. To this end, four boundary conditions at the input and output terminals of the coupled lines are regarded as follows.

$$V_{10}+Z_SI_{10}=V_S \tag{8a}$$

$$V_{1l}-Z_LI_{1l}=0 \tag{8b}$$

$$V_{20}+Z_NI_{20}=0 \tag{8c}$$

$$V_{2l}-Z_FI_{2l}=0 \tag{8d}$$

By considering the mentioned boundary conditions, and four equations in matrix form Equations (7) and (8), the eight unknowns can be calculated by following matrix representation [17].

$$\mathbf{AX}=\mathbf{B} \tag{9a}$$

$$\mathbf{X}=\mathbf{A}^{-1}\mathbf{B} \tag{9b}$$

in which

$$\mathbf{X}=\begin{bmatrix}\mathbf{X}_1 & \mathbf{X}_2\end{bmatrix}^T \tag{10a}$$

$$\mathbf{X}_1=\begin{bmatrix}V_{10} & I_{10} & V_{1l} & I_{1l}\end{bmatrix} \tag{10b}$$

$$\mathbf{X}_2=\begin{bmatrix}V_{20} & I_{20} & V_{2l} & I_{2l}\end{bmatrix} \tag{10c}$$

$$\mathbf{B}=\begin{bmatrix}V_S & 0 & 0 & 0 & 0 & 0 & 0 & 0\end{bmatrix}^T \tag{10d}$$

and

$$\mathbf{A}=\begin{bmatrix}\mathbf{A}_{11} & \mathbf{A}_{12}\\ \mathbf{A}_{21} & \mathbf{A}_{22}\end{bmatrix} \tag{11a}$$

$$\mathbf{A}_{11}=\begin{bmatrix}1 & Z_S & 0 & 0\\ 0 & 0 & 1 & -Z_L\\ 0 & 0 & 0 & 0\\ 0 & 0 & 0 & 0\end{bmatrix} \tag{11b}$$

$$\mathbf{A}_{12}=\begin{bmatrix}0 & 0 & 0 & 0\\ 0 & 0 & 0 & 0\\ 1 & Z_N & 0 & 0\\ 0 & 0 & 1 & -Z_F\end{bmatrix} \tag{11c}$$

$$\mathbf{A}_{21}=\begin{bmatrix}1 & 0 & -T_{11} & -T_{12}\\ 0 & 1 & -T_{21} & -T_{22}\\ 0 & 0 & 0 & -T_{32}\\ 0 & 0 & -T_{41} & 0\end{bmatrix} \tag{11d}$$

$$\mathbf{A}_{22}=\begin{bmatrix}0 & 0 & 0 & -T_{14}\\ 0 & 0 & -T_{23} & 0\\ 1 & 0 & -T_{33} & -T_{34}\\ 0 & 1 & -T_{43} & -T_{44}\end{bmatrix} \tag{11e}$$

For a symmetrical microstrip directional coupler, in which all ports are matched, insertion loss (*IL*), return loss (*RL*), coupling factor (*CF*), and isolation factor (*IF*) are approximately determined by the following closed-form formulas.

$$RL\approx\left(V_{10}-Z_SI_{10}\right)/\left(V_{10}+Z_SI_{10}\right) \tag{12a}$$

$$IL\simeq\exp(-\gamma l)\cosh\left[\left(k_1+k_2\right)l/2\right] \tag{12b}$$

$$CF\approx\frac{k_2-k_1}{4\gamma}\left\{1-\mathrm{e}^{-2\gamma l}\left[\cosh\left(k_1+k_2\right)l-\frac{k_1-k_2}{j\,2\gamma}\sinh\left(k_1+k_2\right)l\right]\right\} \tag{12c}$$

$$IF \approx -\exp(-\gamma l)\sinh\left[\left(k_1+k_2\right)l/2\right] \tag{12d}$$

in which

$$k_1 = \frac{Y_m}{u}\sqrt{\frac{j\omega C_1}{Y_1\left(C_1C_2-C_m^2\right)}} \tag{13a}$$

$$k_2 = \frac{j\omega C_m}{u}\sqrt{\frac{Y_2}{j\omega C_1\left(C_1C_2-C_m^2\right)}} \tag{13b}$$

u in the above equations is wave velocity. It is worth noting that the accuracy of the obtained equations severely depends on the per unit length parameters of the coupled lines. For a symmetrical coupled microstrip line, Equations (14a) and (14b) present an approximation value of per-unit-length parameters [18].

$$\frac{C_1}{\varepsilon} \simeq \left[1.15\left(\frac{W}{H}\right)^{0.963}+1.07\left(\frac{T}{H}\right)^{0.049}\right]+ e^{-3.52\frac{S}{H}}\left[0.75\left(\frac{W}{H}\right)^{0.25}+2.7\left(\frac{T}{H}\right)^{1.36}\right] \tag{14a}$$

$$\frac{C_m}{\varepsilon} \simeq 1.17\left(\frac{W}{H}\right)^{0.083}\left(\frac{S}{H}+0.402\right)^{-0.78}+ \left(\frac{S}{H}+1.32\right)^{-0.8}\left[-1.36\left(\frac{W}{H}\right)^{-0.037}+0.227\left(\frac{T}{H}\right)^{0.98}\right] \tag{14b}$$

3. MICROSTRIP LINE COUPLER DESIGN

In this section, the design process of a backward coupler using a microstrip line placed on a perforated substrate is reported. As stated by Karimian-Sarakhs et al. [19], any two-dimensional perforated substrate is modeled by its equivalent one-dimensional perforated substrate. To this end, the equivalent propagation constant $\gamma_e=\alpha_e+j\beta_e$ is determined by equations (15a) and (15b) [19].

$$\gamma_e = \frac{1}{L_1+L_2}\cosh^{-1}\left[\frac{1-\Lambda}{2}\cosh\left(\sum_{i=1}^{2}(-1)^{i-1}\gamma_i L_i\right)+\frac{1+\Lambda}{2}\cosh\left(\sum_{i=1}^{2}\gamma_i L_i\right)\right] \tag{15a}$$

$$\Lambda = \frac{\varepsilon_1+\varepsilon_2}{\sqrt{\varepsilon_1\varepsilon_2}} \tag{15b}$$

in which (L_1, ε_1, γ_1), (L_2, ε_2, γ_2) are the length, dielectric permittivity, and the propagation constant of dielectric and air sections along the *x*-direction of the perforated substrate, respectively. The α_e and β_e are the equivalent attenuation and phase constant of the substrate. Additionally, the introduced transformation can be applied to any 2-D substrate with arbitrary shapes of air holes. More details are discussed by Karimian-Sarakhs et al. [19].

A microstrip directional coupler based-on 1-D perforated substrate can be regarded as a multi-section directional coupler. For each section, transmission matrix **T** is calculated using Equation (7). Since the coupler is divided into a few series of sub-sections, the total transmission matrix of the coupler is determined by multiplying the transmission matrix of the sub-sections given by Equation (16) [20].

$$\mathbf{T}_t = \prod_{n=1}^{N}\mathbf{T}_n \tag{16}$$

in which $\mathbf{T}_t$, $\mathbf{T}_n$, and N are the total transmission matrix, the transmission matrix of the nth section, and the total number of series sections, respectively. By specifying $\mathbf{T}_t$, the required parameters of the coupler including coupling factor, directivity, insertion loss, and return loss can be evaluated using the provided equations. Since the proposed method is an analytical approach, the desired parameters of the directional coupler can be straightforwardly optimized using well-known algorithms such as genetic algorithm (GA), particle swarm optimization (PSO), and the other methods.

4. RESULTS AND DISCUSSION

The microstrip line on the artificial perforated substrate provides several band gaps in its frequency response, due to existing of air holes in the structure [21]. Hence, the directional couplers established on the perforated substrate have typically low-frequency bandwidth. However, by selecting the proper value of the ratio of the dielectric section length to the air section length (L_1/L_2), the band-gaps is shifted to the undesired frequency band. Figure 2 shows the phase constant of a perforated substrate for different values of ratio L_1/L_2. It can be seen that by increasing the value of L_1/L_2, the first band gaps will be shifted to the lower frequencies. Also, the number of band gaps will be increased with the arising value of L_1/L_2.

Another factor influencing the band-gap properties of a perforated substrate is the length of the dielectric and air sections. Figure 3 shows the phase constant of a perforated substrate for different values of L_1, and L_2. It is worth noting that in this figure, the length of air and dielectric sections are equal. It can be seen that similar to Figure 2, by increasing the length of dielectric and air sections, the first band gap has appeared at lower frequencies. Additionally, the number of band gaps will be also increased by arising the length of dielectric and air sections. As a result, to design a directional coupler based on the perforated substrate, not only L_1 and L_2

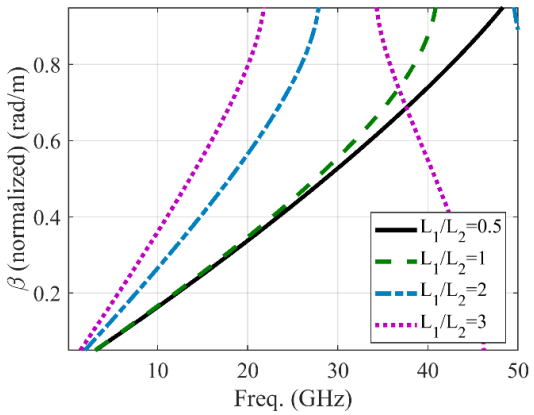

Figure 2. Phase constant of the perforated substrate for different values of ratio L_1/L_2

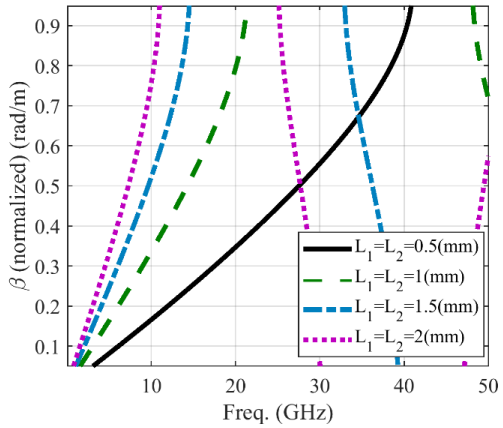

Figure 3. Phase constant of the perforated substrate for different values of L_1, and L_2

should be a small value, but also, L_1, and L_2 should be as small as possible. It should be noted that values of L_1, L_2 should be physically acceptable.

Considering the aforementioned limitations, a microstrip backward directional coupler with a coupling level of 10 dB is designed and investigated based on a perforated substrate with a dielectric permittivity of 10.2, a thickness of 0.635 mm, tangent loss of 0.0035, and conductor thickness 17 μm. The dimensions of the proposed coupler are W_S=3.2 mm, and L_S=2.9 mm as defined in Figures 4(a) and 4(b) including the other geometrical parameters of the two couplers. The primary design is done using the presented formulas in section II, and the final geometrical parameters of determined using an optimization procedure by PSO implemented by MATLAB code. Figure 5 shows the flowchart of the optimization procedure. In the optimization process, a 10 dB coupling level with a maximum ripple of 0.5 dB, and return loss better than 15 dB are considered as the objective and constrains. Also, the minimum and maximum values of the substrate parameters (L_d, L_a, D, d) are determined according to Figures 2, 3, and corresponded expressions. The maximum length of the couplers is considered equal to $\lambda_g/2$. The maximum variations for W and S are about of ±10% around their initial values.

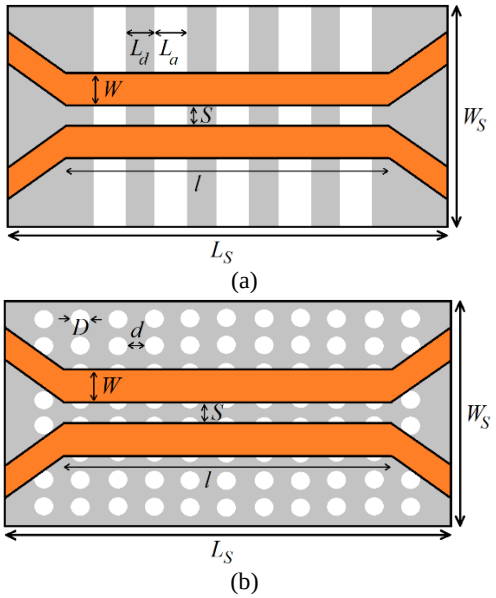

Figure 4. Microstrip backward directional coupler based on (a) 1-D perforated substrate (b) a 2-D perforated substrate

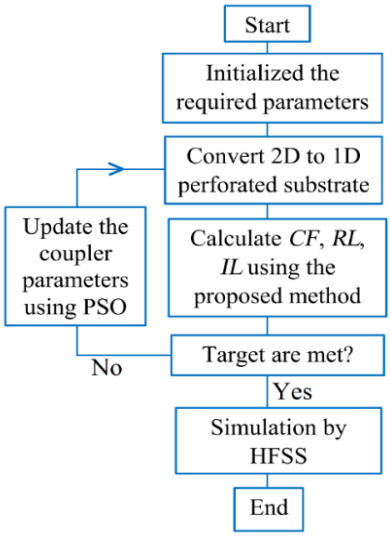

Figure 5. Flowchart of the designed coupler procedure

Figure 6 shows the equivalent attenuation and phase constant of the 1-D and 2-D perforated substrate using the introduced method by Karimian-Sarakhs et al. [19], which confirms that the first band gap is far from the desired frequency band. For the designed couplers, the isolated port is terminated to a 50 Ω load to obtain good return loss. The initial and optimized parameters of the couplers are summarized in Tables 1 and 2.

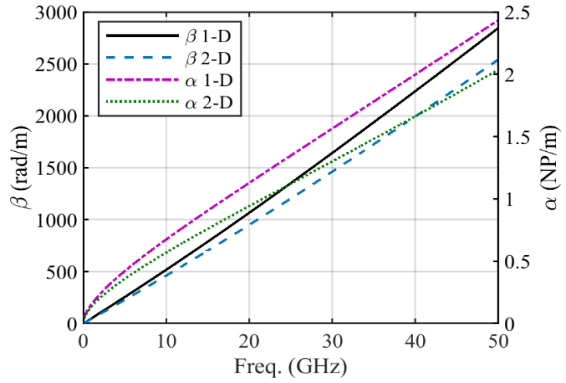

Figure 6. The equivalent attenuation and phase constant of the 1-D and 2-D perforated substrate

TABLE 1. The initial and optimized parameters of the coupler based on a 1-D perforated substrate. (All values in mm)

Parameter	Initial Value	Optimized Value
L_d	0.25	0.1
L_a	0.3	0.1
W	0.5	0.58
S	0.25	0.2
l	1.5	1.1

TABLE 2. The initial and optimized parameters of the coupler based on a 2-D perforated substrate (All values in mm)

Parameter	Initial Value	Optimized Value
D	0.3	0.2
d	0.1	0.3
W	0.5	0.58
S	0.25	0.15
l	1	3

Figure 7 shows the simulation results of scattering parameters of the designed backward coupler using a 1-D perforated substrate. It can be seen that the obtained *RL* is better than 15 dB, while the maximum *IL* is 0.8 dB, and the coupling level is 10 dB. Moreover, the coupling ripple is lower than 0.5 dB in a wide frequency range from 25 GHz to 35 GHz. The coupler bandwidth is 34%. Figure 8, the simulation results of the phase of S_{21}, and S_{31} are depicted, which are linear along the operating bandwidth. Figures 9 and 10 show the results of the designed 10 dB coupler on a non-perforated substrate. These figures show does not provide good performance for the directional coupler on a non-perforated substrate compared to the designed coupler using a perforated substrate.

Figure 11(a) shows the simulation results of the scattering parameters of the designed backward coupler

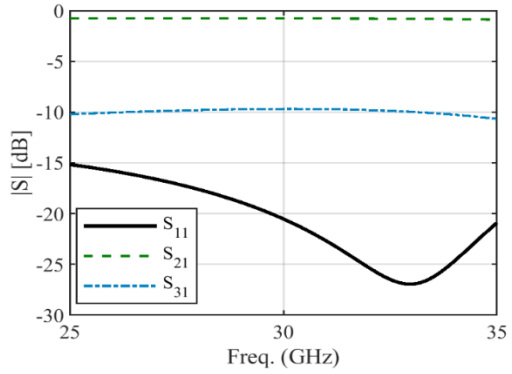

Figure 7. The simulation results of scattering parameters of the designed backward coupler using a 1-D perforated substrate

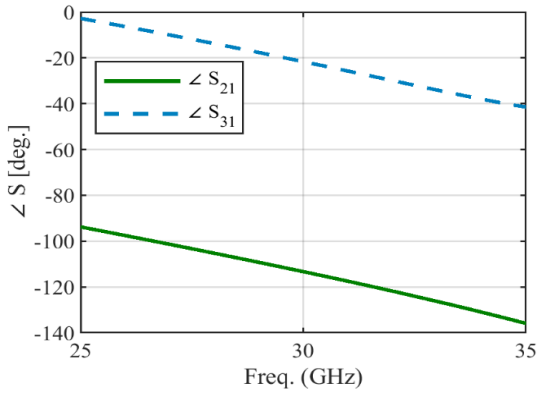

Figure 8. The simulation results of the phase of *S*-parameters of the proposed coupler using a 1-D perforated substrate

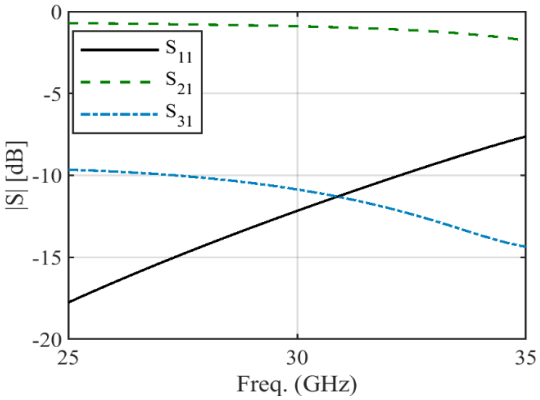

Figure 9. The simulation results of scattering parameters of the designed backward coupler using a non-perforated substrate.

using a 2-D perforated substrate. It can be seen that *RL* is better than 15 dB, and the maximum *IL* is 1 dB. Figure 11(b) also shows that the coupler flatness is less than 0.5 dB in the wide frequency range from 32 GHz to 38 GHz.

The obtained bandwidth is about 17% at a center frequency of 35 GHz. Figure 12, also, shows the simulation results of the phase of the scattering parameters including S_{21} and S_{31} versus frequency. It can be seen that the phases of S_{21}, and S_{31} are linear along the operating bandwidth. Furthermore, Figures 13 and 14 show the results of the same 2-D coupler using a non-perforated substrate. It can be seen that the performance of the directional coupler on a non-perforated substrate is weaker than the designed coupler using a perforated substrate.

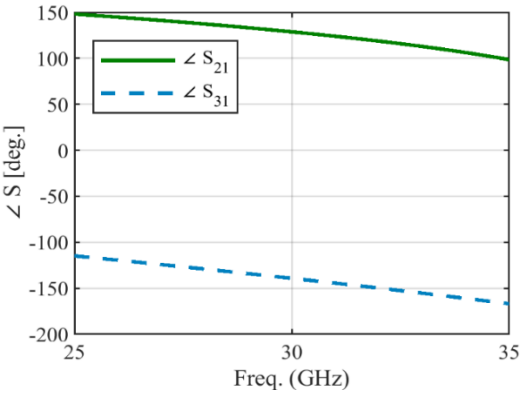

Figure 10. The simulation results of the phase of *S*-parameters of the coupler using the non-perforated substrate

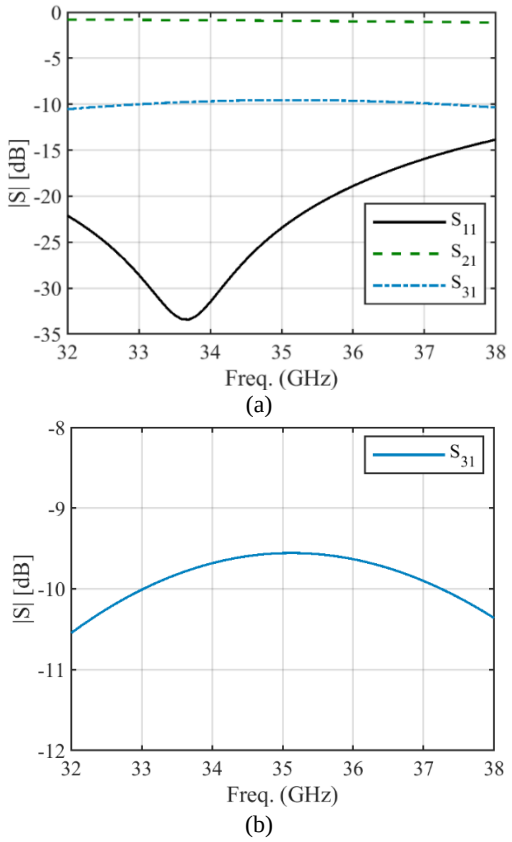

Figure 11. The simulation results **a.** scattering parameters of the designed backward coupler using a 2-D perforated substrate **b.** S_{31} and flatness of the designed backward coupler using a 2-D perforated substrate

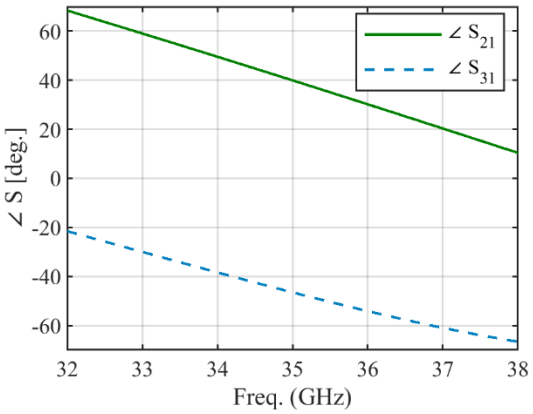

Figure 12. The simulation results of the phase of *S*-parameters of the proposed coupler using a 2-D perforated substrate

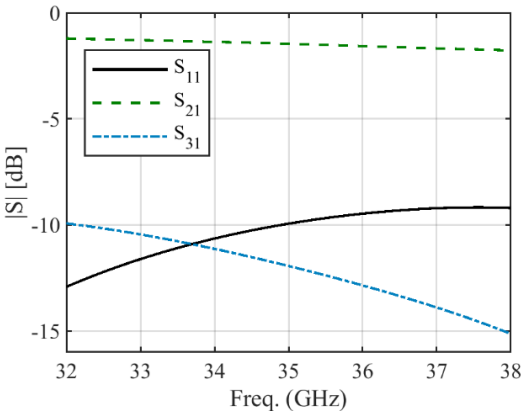

Figure 13. The simulation results of the same 2-D coupler using a non-perforated substrate

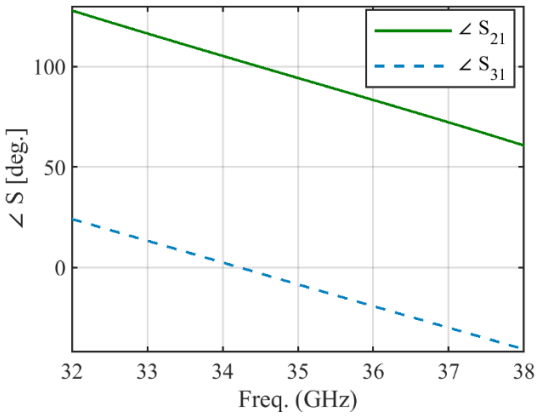

Figure 14. The simulated results of the phase of S-parameters for a coupler using a non-perforated substrate

The detailed performance of the proposed couplers and the simulated results of the recently published research, including center frequency f_0, coupling level *CF*, coupling ripple in pass band, total size, coupler bandwidth *BW*, average *IL*, and maximum *RL* are reported in Table 3. This table confirms that for a 10 dB level of coupling, the proposed coupler using the 2-D perforated substrate provides the lowest *IL* with a 17% bandwidth while the coupler size is only $0.32\times0.29\lambda^2_g$.

5. SENSITIVITY ANALYSIS

In order to study the effects of fabrication imperfection on the performance of the proposed couplers, a sensitivity analysis is carried out using random error by uniform distribution with 0 average for the geometrical parameters of the structure in Tables 1 and 2. The standard deviation is chosen in such a way that these parameters are changed over a maximum variation range of ±10% around the central value. To this end, the introduced method by Trinchero et al. [22] is employed. Figures 15, and 16 show the obtained results for the 1-D and 2-D couplers based on the perforated substrate. In these figures, the uncertain area is depicted by gray color. Also, the simulation results of S_{11}, S_{21}, and S_{31} are shown by back, blue and red lines, respectively. For the 1-D coupler, the maximum deviation of S_{11}, S_{21}, and S_{31} from the simulation ones are about 3.1 dB, 0.1 dB, and 0.52 dB, respectively. Also, for the 2-D coupler, the maximum deviation of S_{11}, S_{21}, and S_{31} from the simulation ones are about 6.9 dB, 0.1 dB, and 0.53 dB, respectively. It is seen that the value of S_{11} is more affected.

6. CONCLUSION

In this paper, at first, the coupled version of the transmission line equation of two microstrip lines is derived and then, the extended version of the *ABCD* matrix of a four ports microwave network is introduced using the closed-form expression. Two low-profile microstrip backward directional couplers placed on a 1-D and 2-D artificial perforated substrate are designed using the proposed analytical method. Using an optimization procedure by PSO, the optimum

TABLE 3. The detailed simulated performances of the proposed couplers and those recently published in literature

	Number of Layers	f_0 (GHz)	Ripple (dB)	*CF* (dB)	*IL* (dB)	*RL* (dB)	*BW* (%)	Coupler size ($\lambda_g\times\lambda_g$)
[6]	2	26	2	5	5	11	15.7	3.8×0.5
[7]	3	30	2.3	5	2.5	15	26	1.2×1.2
[9]	2	60	1	10	0.5	20	33	9.8×4.8
[11]	1	35	1.2	3	5	17	28	3.55×1.92
[12]	2	30	1.4	5	5	7	14	1.12×1.12
This work	1 (1-D*)	30	0.6	10	0.8	15	34	0.5×0.11
	1 (2-D*)	30	1	10	0.9	17	27	0.32×0.29
	1 (2-D)	35	0.5	10	1	15	17	0.32×0.29

*) These couplers are used without connectors or bending.

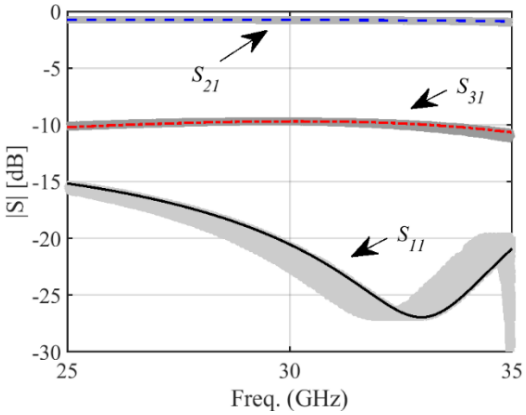

Figure 15. The sensitivity analysis of 1-D couplers based on the perforated substrate

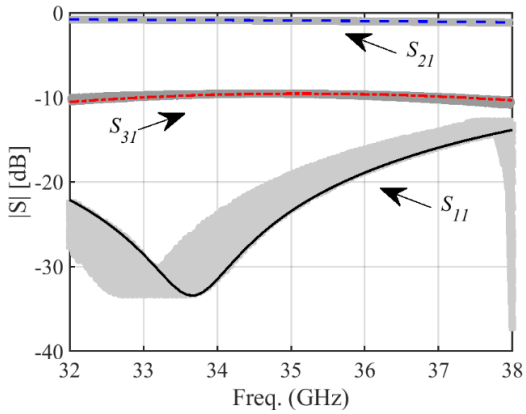

Figure 16. The sensitivity analysis of 2-D couplers based on the perforated substrate

geometrical dimensions of both couples are determined. The proposed couplers are simulated using HFSS software and their performances including scattering parameters, insertion loss, and coupler flatness are reported. Results show that the operating frequency band of the couplers are 25-35 GHz and 32-38 GHz for 1-D and 2-D substrates, respectively. The obtained results of the couplers show a good performance with low insertion, high return loss, and wide operating bandwidth.

7. REFERENCES

1. Fonseca, N. J. G., Angevain, J. C., "Waveguide Hybrid Septum Coupler," ***IEEE Transactions on Microwave Theory and Techniques***, Vol. 69, No. 6, (2021), 3030-3036. https://doi.org/ 10.1109/TMTT.2021.3074194
2. Tabatabaeian, Z. S., Neshati, Mohammad H., "Sensitivity Analysis of a Wideband Backward-wave Directional Coupler Using Neural Network and Monte Carlo Method," ***International Journal of Engineering Transaction B Applications***, Vol. 31, No. 5, (2018), 729-733.
3. Alcep, A., Tokan, F., "Perforated Dielectric Lens Antenna Design," ***International Journal on Future Revolution in Computer Science & Communication Engineering***, Vol. 4, No. 12, (2018), 12-15.
4. Wang, Z.B., Wei, X., Fang, H.P., Zhang, H.M., Zhang, Y.R., "A Compact and Broadband Directional Coupler for High-Power Radio Frequency Applications," ***IEEE Microwave and Wireless Components Letters***, Vol. 30, No. 2, (2020), 164-166. https://doi.org/ 10.1109/LMWC.2020.2964672
5. Sedaghat, M., Firouzeh, Z.H., Aliakbarian, H., "Development of a Non-Iterative Macro-Modelling Technique by Data Integration and Least Square Method," ***International Journal of Engineering Transaction B Applications***, Vol. 34, No. 11, (2021), 2408-2417. https://doi.org/ 10.5829/ije.2021.34.11b.04
6. Cao, Y., Wu, Y., Jiang, Z., Hao, Z., "A Compact Millimetre-Wave Planar Directional Coupled Crossover with a Wide Bandwidth," ***IEEE Microwave and Wireless Components Letters***, Vol. 30, No. 7, (2020), 661-664. https://doi.org/ 10.1109/LMWC.2020.2998780
7. Ali, M. M. M., El-Gendy, M. S., Al-Hasan, M., Mabrouk, I. B., Sebak, A., Denidni, T.A., "A Systematic Design of a Compact Wideband Hybrid Directional Coupler Based on Printed RGW Technology," ***IEEE Access***, Vol. 9, (2021), 56765-56772. https://doi.org/ 10.1109/ACCESS.2021.3071758
8. Parment, F., Ghiotto, A., Vuong, T., Duchamp, J., Wu, K., "Air-to-Dielectric-Filled Two Hole Substrate-Integrated Waveguide Directional Coupler," ***IEEE Microwave and Wireless Components Letters***, Vol. 27, No. 7, (2017), 621-623. https://doi.org/ 10.1109/LMWC.2017.2711525
9. Zarifi, D., Farahbakhsh, A., Zaman, A. U., "Design and Fabrication of Wideband Millimetre-Wave Directional Couplers with Different Coupling Factors Based on Gap Waveguide Technology," ***IEEE Access***, Vol. 7, (2019), 88822-88829. https://doi.org/ 10.1109/ACCESS.2019.2926233
10. Peláez-Pérez, A. M., Almorox-Gonzalez, P., Alonso, J.I., González-Martín, J., "Ultra-Broadband Directional Couplers Using Microstrip with Dielectric Overlay in Millimetre-Wave Band," ***Progress in Electromagnetics Research***, Vol. 117, (2011), 495-509. https://doi.org/ 10.2528/PIER11042703
11. Tavakoli, M. J., Mallahzadeh, A., "Wideband Directional Coupler for Millimetre Wave Application based on Substrate Integrated Waveguide," ***Emerging Science Journal***, Vol. 2, No. 2, (2018). https://doi.org/ 10.28991/esj-2018-01132
12. Zhao, Z., Denidni, T. A., "Millimetre-Wave Printed-RGW Hybrid Coupler with Symmetrical Square Feed," ***IEEE Microwave and Wireless Components Letters***, Vol. 30, No. 2, (2020), 156-159. https://doi.org/10.1109/LMWC.2019. 2960475
13. Tabatabaeian, Z. S., Neshati, Mohammad H., "Development of broadband forward-wave directional couplers loaded by periodic patterned ground structure," ***International Journal of RF and Microwave Computer-Aided Engineering***, Vol. 27, No. 8, (2017), 1-9. https://doi.org/ 10.1002/mmce.21135
14. Tabatabaeian, Z.S., Neshati, Mohammad H., "Development of Forward-wave Directional Couplers Loaded by Periodic Shunt Shorted Stubs," ***International Journal of Engineering Transaction C Aspect***, Vol. 30, No. 3, (2017), 344-350. https://doi.org/10.5829/idosi.ije.2017.30.03c.03
15. Pozar, D. M., Microwave Engineering. John Wiley & Sons, 4th e, 2011.
16. Paul, C. R., Introduction to Electromagnetic Compatibility. 2nd ed., 2006.
17. Strang G., Introduction to Linear Algebra. Cambridge Press, 2016.
18. Sohn, Y. S., Lee, J,C., Park, H.J., Cho, S.I., "Empirical equations on electrical parameters of coupled microstrip lines for crosstalk estimation in printed circuit board," ***IEEE Transactions on Advanced Packaging***, Vol. 24, No. 4, (2001), 521–527. https://doi.org/ 10.1109/6040.982839
19. Karimian-Sarakhs, H., Neshati, Mohammad H., and Alijani, M. G. H., "Development of an analytical method to determine the propagation characteristics of microstrip line on artificial perforated substrates," ***AEU-International Journal of Electronics and Communications***, Vol. 140, (2021), 1-8. https://doi.org/ 10.1016/j.aeue.2021.153951
20. Alijani-Ghadikolae, M., Neshati, Mohammad H., "Developing an accurate and simple dispersion analysis of TE10 mode of substrate integrated waveguides," *21st Iranian Conference on Electrical Engineering (ICEE)*, (2013), 1-4. https://doi.org/ 10.1109/IranianCEE.2013.6599879
21. Méndez-Jerónimo, G., Wu, K., "Effects of Unshielded Air Holes Periodically Perforated in Substrate Integrated Waveguides," ***IEEE Microwave and Wireless Components Letters***, Vol. 30, No. 11, (2020), 1049-1052. https://doi.org/ 10.1109/LMWC.2020.3022973.
22. Trinchero, R., Manfredi, O., Stievano, I.S., Canavero, F.G., "Machine Learning for the Performance Assessment of High-Speed Links," ***IEEE Transactions on Electromagnetic Compatibility***, Vol. 60, No. 6, (2018), 1627-1634. https://doi.org/ 10.1109/TEMC.2018.2797481.

Persian Abstract

چکیده

در این مقاله، دو تزویج کننده جهتی معکوس پهن باند با ضریب تزویج ۱۰ دسی بل مبتنی بر زیرلایه حفره دار در محدوده فرکانس ۲۵–۳۵ گیگاهرتز و ۳۲–۳۸ گیگاهرتز توسعه داده شده است. یک روش تحلیلی برای طراحی پارامترهای هندسی کوپلر پیشنهاد شده است. مدل سازی نظری بر اساس تئوری خط انتقال با استفاده از نسخه توسعه یافته ماتریس ABCD برای شبکه مایکروویو چهار پورت ارائه شده است. نشان داده شده است که با استفاده از روش پیشنهادی، تمام پارامترهای مورد نیاز کوپلر جهتی را می توان با استفاده از پارامترهای واحد طول خط تعیین کرد. برای بهبود عملکرد کوپلرهای طراحی شده از الگوریتم بهینه سازی ذرات برای بهینه سازی پارامترهای هندسی کوپلرها استفاده شده است. همچنین، کوپلرهای طراحی شده با استفاده از شبیه ساز ساختار فرکانس بالا (HFSS) شبیه سازی شده اند. علاوه بر آن، برای بررسی تاثیر ناکاملی در فرآیند ساخت، تحلیل حساسیت نیز به کار گرفته شده است. نتایج به‌دست‌آمده نشان می‌دهد که نتایج شبیه‌سازی به خوبی با نتایج نظری مطابقت دارد و تلفات تعبیه کم به همراه تلفات بازگشتی زیاد در پهنای باند فرکانسی وسیع به‌دست می‌آید.